Systematics of x-ray resonant scattering amplitudes in $R\mathrm{Ni}_2\mathrm{Ge}_2$: The origin of the branching ratio at the L edges of the heavy rare-earths

J.W. Kim, Y. Lee, D. Wermeille, B. Sieve, L. Tan, S. Law, S.L. Bud'ko, P.C. Canfield, B.N. Harmon and A.I. Goldman
Ames Laboratory USDOE and the Department of Physics and Astronomy, Iowa State University, Ames IA 50011

Deciphering the information contained in XMCD and XRMS amplitudes, and relating these amplitudes to the details of the electronic and magnetic structure of the material, are important, but difficult tasks. Over the past few years, one of the most intriguing issues has been the so-called branching ratio problem in the rare-earth elements.[1] Measurements of the ratio of the L_3/L_2 resonant scattering intensity consistently show that the L_3 edge intensities are significantly larger than the corresponding L_2 edge intensities for the heavy rare-earth elements, whereas the inverse is true for the light rare-earths. Since the resonant scattering cross-section and XMCD amplitude are closely related, the same effect is observed in the relative amplitudes of XMCD measurements at the L_2 and L_3 edges of rare earth compounds. Spin-polarized band structure calculations which include only the $4f$-$5d$ exchange interaction (no conduction-band SOC or $4f$ orbital polarization), produce a branching ratio across the entire rare-earth series equal to unity (1:1 for XRMS and 1:-1 for XMCD). Atomic models,[3, 4] with parameterized $5d$ orbitals, have met with some success in explaining the branching ratios observed in $R_2\mathrm{Fe}_{17}$, for example, by including $4f$ orbital polarization and introducing "breathing" (a contraction of the spin-up radial function relative to the spin-down radial function) of the $5d$ orbitals. This increases the overlap of the $5d$ spin-up states with the $2p$ core states, as first shown by Harmon and Freeman.[5] Being primarily atomic models, however, they do not include the strong dependence of the radial functions on band energies (e.g. the bonding and antibonding $5d$ states differ in their $4f$-$5d$ exchange by more than a factor of two). In spite of these studies, the origin of the variation of the branching ratio in rare-earth compounds remains problematical,[2] and the extension of current treatments of both XRMS and XMCD amplitudes to extract compound specific magnetic property information remains a priority.

Here, we take an important step in addressing this issue through a systematic study of the XRMS branching ratio at the L edges of heavy rare-earths in $R\mathrm{Ni}_2\mathrm{Ge}_2$ compounds for R = Gd through Tm. Our approach involves exploiting the fact that similarities in the chemistry of rare-earth elements across the series allow the easy substitution of one rare-earth element for another in isostructural compounds. Since the resonant scattering at each absorption edge is element-specific, probing the systematics of resonant scattering associated with several different rare-earth elements is possible using only a few mixed rare-earth samples. This helps to reduce the uncertainty in the measurements arising from variations in quality and mosaic from sample-to-sample. Further, the relatively straightforward incommensurate antiferromagnetic structure found at low temperature in the $R\mathrm{Ni}_2\mathrm{Ge}_2$ family of compounds has been the subject of prior XRMS and single-crystal neutron scattering investigations [6] as well as polycrystalline neutron measurements.[7]

Single crystals of $[\mathrm{Gd}_{1/3}\mathrm{Er}_{1/3}\mathrm{Tm}_{1/3}]\mathrm{Ni}_2\mathrm{Ge}_2$ and $[\mathrm{Gd}_{1/4}\mathrm{Tb}_{1/4}\mathrm{Dy}_{1/4}\mathrm{Ho}_{1/4}]\mathrm{Ni}_2\mathrm{Ge}_2$ were produced at the Ames Laboratory using the high-temperature solution-growth technique.[8, 9] The $R\mathrm{Ni}_2\mathrm{Ge}_2$ family crystallizes in the body-centered tetragonal $\mathrm{ThCr}_2\mathrm{Si}_2$ structure with space group $I4/mmm$ (D_{4h}^{17}). The Wyckoff positions of the rare earth ion (R) are $2(a)$ with point symmetry D_{4h}. The $R\mathrm{Ni}_2\mathrm{Ge}_2$ compounds order antiferromagnetically, via the indirect exchange (RKKY) interaction, below Néel temperatures (T_N) ranging from 1.5 K for Tm to 27.1 K for Gd.[9] The values of T_N for the mixed rare-earth samples used in this experiment were approximately 12 K for both compounds. The moderate value of T_N, together with the absence of additional magnetic transitions in the bulk susceptibility measurements of the samples is consistent with a random distribution of the rare-earth elements on the $2(a)$ sites.

XRMS measurements were performed on the 6ID-B beam line in the MUCAT Sector at the Advanced Photon Source with the incident radiation linearly polarized perpendicular to the scattering plane (σ-polarization). In this geometry, only the component of the magnetic moment that is in the scattering plane will contribute to the resonant scattering arising from electric dipole transitions from the $2p$-to-$5d$ states. The linear polarization of the scattered radiation for dipole resonant scattering is parallel to the scattering plane (π-polarization). A pyrolytic graphite analyzer PG(0 0 6), optimized to select primarily π-polarized radiation was used to reduce the background from charge scattering.

For each of the two samples, the XRMS intensity was recorded at all of the rare earth L_2 and L_3 absorption edges over a range of approximately ± 25 eV about the absorption edge energy. At each energy, the integrated intensity of the magnetic satellite at $(0\ 0\ 6+\tau_z)$ was obtained with a rocking scan through the sample mosaic. The same procedure was used to obtain backgrounds for the energy spectra above the respective T_N for each sample. In order to extract and compare the resonant scattering intensities at the various edges, separated by several

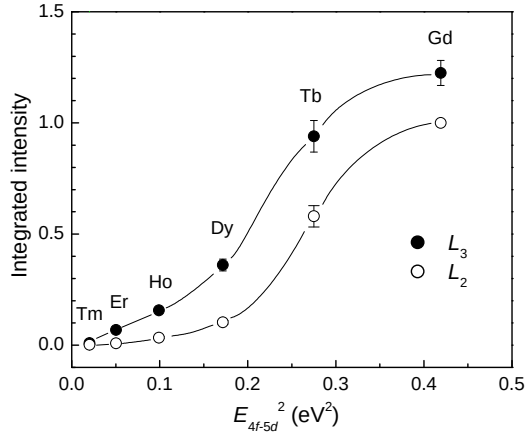

FIG. 1: The fit value of the integrated intensity of the resonant magnetic scattering, $E_0^4(F_{11} - F_{1-1})^2$, at the L_2 (open circles) and L_3 edges (closed circles) for both samples, plotted as a function of the square of the $4f$-$5d$ exchange energy. The data are normalized to the integrated intensity at the Gd L_2 edge of the samples. The solid lines serve as a guide to the eye.

keV in energy, careful account must be taken of sample and beam line absorption factors over the entire energy range. These energy dependent corrections were obtained through energy scans over the range of interest with powders of the two samples. In addition, the throughput of the beam line optics and the polarization analyzer were measured over the entire energy range.

The importance of the $4f$-$5d$ exchange is highlighted in Fig. 1 where we plot the normalized XRMS integrated intensities at the L_2 and L_3 edges as a function of the square of the atomic $5d$ exchange energy splitting for the rare-earth elements. There is a striking enhancement of the resonant scattering intensity as the $4f$-$5d$ exchange interaction increases from Tm to Gd, and this change across the series is consistent with previous studies highlighting the importance of the $4f$-$5d$ exchange relative to other solid state effects. In particular, for Gd, with seven unpaired $4f$ electrons, the on-site $4f$-$5d$ exchange interaction is largest and dominates over other interactions. Hence, we expect the L_2 and L_3 spectra for Gd to be only weakly affected by the specific crystalline environment. However, as one proceeds along the heavy rare earth series the number of unpaired $4f$ electrons decreases, so that for Ho, Er, and Tm the $5d$ spin-orbit coupling and even crystal electric field interactions induce comparable, or greater, effects on the resonant scattering amplitude. Indeed, these rare-earth elements may provide useful probes of local environments if various sensitive features in the L_2 and L_3 spectra can be related to the fundamental interactions.

If the normalized integrated intensity of the magnetic scattering at the L_3 edge is divided by the normalized integrated intensity of the magnetic scattering at the

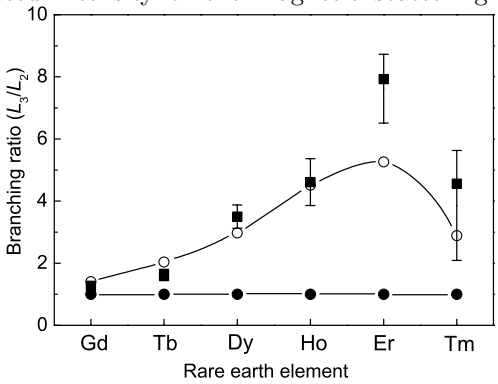

FIG. 2: The XRMS branching ratio for the heavy rare-earth elements in RNi$_2$Ge$_2$ compounds. The solid squares represent the ratio of intensities from the L_2 and L_3 edges shown in Fig. 1. The bars represent the experimental errors as well as the contribution of the quadrupole transition. The solid circles show the result of the first principles calculations ignoring SOC in the $5d$ band. The open circles show the results of the same calculations, now including the effect of spin-orbit coupling in the $5d$ band.

L_2 edge, the branching ratio, plotted as solid squares in Fig. 2, is obtained. The trends observed in the branching ratio as one moves across the heavy rare-earth elements in these measurements are consistent with the first-principles spin-polarized band structure calculations with SOC in the $5d$ band.

[1] See, for example, D. Gibbs, J.P. Hill, and C. Vettier in *Third Generation Hard X-ray Sources: Source Properties, Optics, and experimental techniques*, ed. D. Mills (John Wiley and Sons, Inc, 2002), p. 267.
[2] C. Giorgetti *et al.*, Phys. Rev. B **70**, 035105 (2004).
[3] M. van Veenendaal *et al.*, Phys. Rev. Lett. **78**, 1162 (1997).
[4] K. Fukui*et al.*, J. Electron Spectrosc. Relat. Phenom. **104**, 67 (1999).
[5] B. N. Harmon and A. J. Freeman, Phys. Rev. B **10**, 1979 (1974); B. N. Harmon and A. J. Freeman, Phys. Rev. B **10**, 4849 (1974).
[6] Z. Islam *et al.*, Phys. Rev. B **58**, 8522 (1998); Z. Islam *et al.*, Phys. Rev. Lett. **83**, 2817 (1999); Z. Islam *et al.*, Solid State Commun. **108**, 371 (1998).
[7] H. Pinto *et al.*, Phys. Rev B **31**, 508 (1985).
[8] P.C. Canfield and Z. Fisk, Phil. Mag. B **56**, 1117 (1992).
[9] S.L. Bud'ko *et al.*, J. Magn. Magn. Mater. **205**, 53 (1999).
[10] C. Detlefs *et al.*, Phys. Rev. B **55**, R680 (1997).
[11] J.W. Kim *et al.*, to be published.
[12] D. Gibbs *et al.*, Phys. Rev. B **43**, 5663 (1991).
[13] J.P. Hannon *et al.*, Phys. Rev. Lett. **61**, 1245 (1988).
[14] J.P. Hill and D.F. McMorrow, Acta Crystallogr. **A52**, 236 (1996).